Additive Manufacturing: Metallurgy, Cut Analysis & Porosity

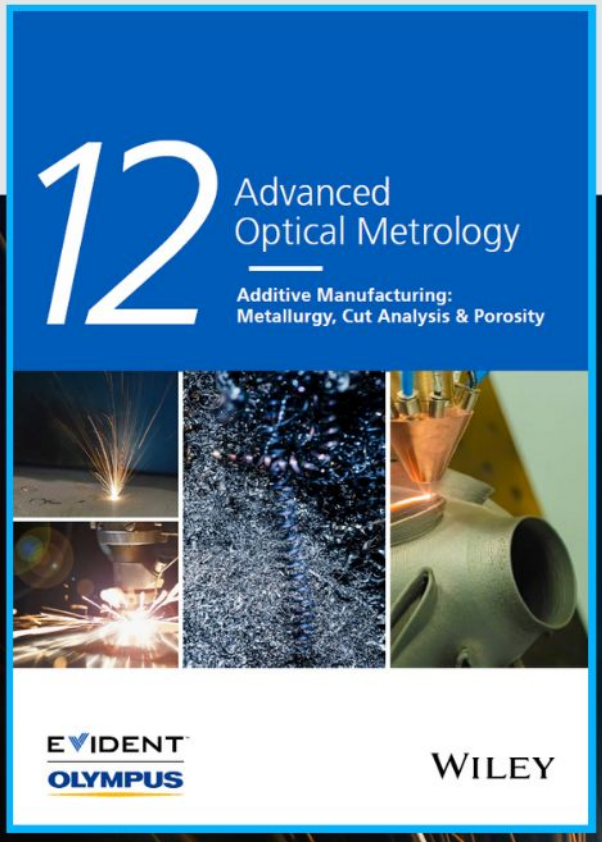

The latest eBook from Advanced Optical Metrology. Download for free.

In industry, sector after sector is moving away from conventional production methods to additive manufacturing, a technology that has been recommended for substantial research investment.

Download the latest eBook to read about the applications, trends, opportunities, and challenges around this process, and how it has been adapted to different industrial sectors.

EVIDENT
OLYMPUS

WILEY

Received: 5 August 2022 | Accepted: 24 August 2022

DOI: 10.1002/maco.202213476

ARTICLE

Materials and Corrosion

The effect of the saliva formulation on brass corrosion

Deborah Biggio | **Bernhard Elsener** | **Davide Atzei** | **Antonella Rossi** | **Marzia Fantauzzi**

Dipartimento di Scienze Chimiche e Geologiche, Università di Cagliari, Cagliari, Italy

Correspondence
Antonella Rossi and Marzia Fantauzzi, Dipartimento di Scienze Chimiche e Geologiche, Università di Cagliari, 09042 Cagliari, Italy.
Email: rossi@unica.it and fantauzzi@unica.it

Funding information
Università di Cagliari; Regione Autonoma della Sardegna, Grant/Award Number: Ph.D. Fellowship of Ms. Biggio; Fondazione di Sardegna, Grant/Award Number: 2019–CUPF72F20000240007; Ministero dell'Università e della Ricerca, Grant/Award Number: POR FSE 2014/2020

Abstract

The composition of natural saliva is strongly variable and unstable outside the oral cavity, therefore corrosion tests are usually performed in artificial saliva solutions. In this study the effect of the composition of various saliva solutions on the corrosion behavior of a CuZn37 alloy, exposed for 1, 3, and 16 h to the solutions, is investigated by using electrochemical measurements, optical microscopy, and X-ray photoelectron spectroscopy (XPS). The solutions investigated in this study are: Darvell, Carter-Brugirard, and SALMO, selected for their composition that mainly differs in the organic compounds' content. Electrochemical measurements show that the open circuit potential and the polarization resistance increase with exposure time in the solutions, indicating a decrease in the corrosion rate. The corrosion rate (μm/year) in the Darvell solution is found to be two times higher than the other artificial saliva formulations and varies in the order: Darvell > Carter-Brugirard > SALMO. These data suggest that the presence of different organic compounds might limit the formation of a stable protective surface film as confirmed by XPS surface analyses.

KEYWORDS
artificial saliva, brass, corrosion, surface films, XPS

1 | INTRODUCTION

Model solutions of human saliva are used for investigating the corrosion behavior of various materials from steels to brass alloys in a wide range of applications, which includes orthodontics and cultural heritage.[1–6] The use of model solutions is required since the natural saliva is a complex mixture of organic and inorganic compounds, strongly variable from person to person as its composition depends on environmental, physiological, and pathological factors.[7–12] In addition, its composition changes throughout the day and, due to its instability outside the oral cavity, it is not usually used for in vivo and in vitro studies.[7,8] So far, several formulations of artificial saliva were proposed for electrochemical studies on alloys used in orthodontics. One of the most common is Tani-Zucchi's formulation,[13] which was recently employed for the investigation of the corrosion behavior of steels exploited in the production of orthodontic appliances[1] and for highlighting the surface modifications induced when musicians play brass wind instruments of historical-artistic interest, belonging to museum collections.[2–6]

Tani-Zucchi has one of the simplest saliva formulations reported in the literature, it contains KSCN, $NaHCO_3$, KCl and NaH_2PO_4, and urea and α-amylase as organic compounds. It is known that organic compounds can form complexes with the metal cations and thus there is the need to ascertain whether the presence of other inorganic compounds and/or if the simultaneous presence in the solution of organic compounds that are also typically revealed in natural human saliva, might play a role in the stability of metal alloys. The results obtained by some of the authors showed that in Tani-Zucchi's solution, the dissolution mechanism of brass alloys was under anodic control, the corrosion rate decreased with prolonged exposure time, and the dissolution rate was controlled by the resistance of the protective film formed on the surface, mainly constituted of CuSCN and $Zn_3(PO_4)_2$.[2–6]

In this study the effect of the composition of various model solutions on the corrosion behavior of a CuZn37 alloy was investigated. The solutions employed in this study are: Darvell (D),[14] Carter-Brugirard (C-B),[15] and SALMO (S),[16] which are characterized by the presence of chlorides, thiocyanates, phosphates, carbonates, and urea. In addition, D solution contains lactic acid, trisodium citrate, and uric acid and, S solution contains glycine. The resistance against corrosion was evaluated by measuring the open circuit potential (OCP), polarization resistance (*R*p), and potentiodynamic polarization curves. Morphological characterization was carried out by optical microscopy and the films grown on the sample surfaces were characterized by X-ray photoelectron spectroscopy (XPS).[17]

2 | MATERIALS AND METHODS

2.1 | Materials and surface preparation

In this study brass alloy CuZn37 samples (Brütsch/Rüegger Werkzeuge AG) were examined. Before the electrochemical measurements, the samples were polished with diamond paste to a mirror-like finish according to the procedure described in Supporting Information: Table S1. This procedure ensured that the starting surface is similar in roughness and composition when exposing the sample to the various solutions. The mechanically polished samples were dried under an argon stream and transferred and analyzed by XPS before and after the exposure to model solutions for electrochemical tests. The transfer took always less than 4 min and a low vacuum vessel was used for the transport of the samples.

2.2 | Model solutions

The saliva formulations used in this study are D, C-B, and S.[14–16] Their chemical composition is provided in Supporting Information: Table S2. D and C-B are colorless solutions, while the S solution is turbid with suspended white particles. The solution pH is 6.81 (0.01), 7.26 (0.02), and 8.06 (0.01), respectively. The measurements are averaged over three independent measurements and the standard deviations are reported in parentheses following the symbolism proposed by EURACHEM.[18] Double-distilled water with a specific conductivity of $1.1 \pm 0.1\,\mu S\,cm^{-1}$ at 293.16 K was used to make up the solutions.

2.3 | Optical microscopy

The optical micrographs of the brass surfaces were obtained using an optical microscope Zeiss, Axiolab A. The microscope is equipped with a camera connected to a computer that allows saving the images taken at various magnifications.

2.4 | Electrochemical tests

Electrochemical tests were carried out in a three-electrode cell described in Corbu et al.[19,20] by using a potentiostat/galvanostat model VersaSTAT3 (Ametek Scientific Instruments Inc.), with a platinum counter electrode and a saturated calomel reference electrode ($E = +0.241$ V vs. NHE). All potentials are referred to as the saturated calomel electrode (SCE). The measurements were performed at room temperature, that is, at 298.2 ± 0.1 K, and the experiments were repeated at least three times.

2.5 | OCP and linear polarization resistance (LPR)

The CuZn37 samples were exposed for 1, 3, and 16 h to the three different model solutions open to the air, and the OCPs were measured. At the end of OCP measurements, the *R*p was determined by imposing a small polarization ±20 mV versus OCP. The scan rate was $0.2\,mV\,s^{-1}$.

2.6 | Cathodic and anodic polarization curves

Cathodic and anodic polarization curves were acquired at a scan rate of $0.2\,mV\,s^{-1}$ following 1 h of immersion time

at OCP. The scan was started by applying a potential of −250 mV versus OCP for the cathodic region and then run to +250 mV versus OCP for the anodic potentiodynamic curves. The anodic (βa) and cathodic (βc) constants were extrapolated from the curves using Versa studio software.[21]

2.7 | XPS surface analysis

Surface composition was investigated by XPS using a ThetaProbe spectrometer (Thermo Fisher Scientific). Survey spectra were acquired with a monochromatic AlKα source (1486.6 eV) and a spot size of 400 µm. The pass energy was set at 200 eV and the step size was 1 eV. The spectrometer was calibrated according to ISO 15472:2010 with an accuracy of ±0.1 eV. Data were processed with CASA XPS software (v2.3.24, Casa Software Ltd.) as described in Cocco et al.[22]

3 | RESULTS

3.1 | Surface morphology

The surface of the samples before the contact with the model solutions was mirror-like finished and it only showed a few scratches due to polishing compared to the as-received samples (Supporting Information: Figure S1a,b). Following the immersion into the model solutions, the contact area of the brass surfaces was opaque and the presence of a film was clearly visible as shown in the micrographs (Supporting Information: Figure S1c–h). The samples exposed to the D solution (Supporting Information: Figure S1c,d) showed the presence of crystallites that appeared to increase in size with exposure time. Crystallites were not observed on the samples exposed to C-B and S solutions (Supporting Information: Figure S1e–h).

3.2 | Electrochemical results

3.3 | OCP

After mechanical polishing, the OCP of the CuZn37 alloy was measured for 1, 3, and 16 h of immersion in solutions open to air. The average values of the potentials versus time of CuZn37 brass exposed for 1, 3, and 16 h to the different solutions are reported in Table 1.

TABLE 1 Average of the initial (E_0) and after 1 h (E_{1h}), 3 h (E_{3h}), and 16 h (E_{16h}) open circuit potential (OCP) values (mV vs. SCE) of CuZn37 exposed to model solutions

Model solutions	OCP vs. SCE (mV)			
	E_0	E_{1h}	E_{3h}	E_{16h}
Darvell	−293 (11)	−327 (1)	−311 (8)	−285 (18)
Carter-Brugirard	−301 (13)	−311 (1)	−303 (17)	−164 (6)
SALMO	−309 (5)	−282 (2)	−277 (19)	−190 (15)

Note: Standard deviations are given in parentheses.

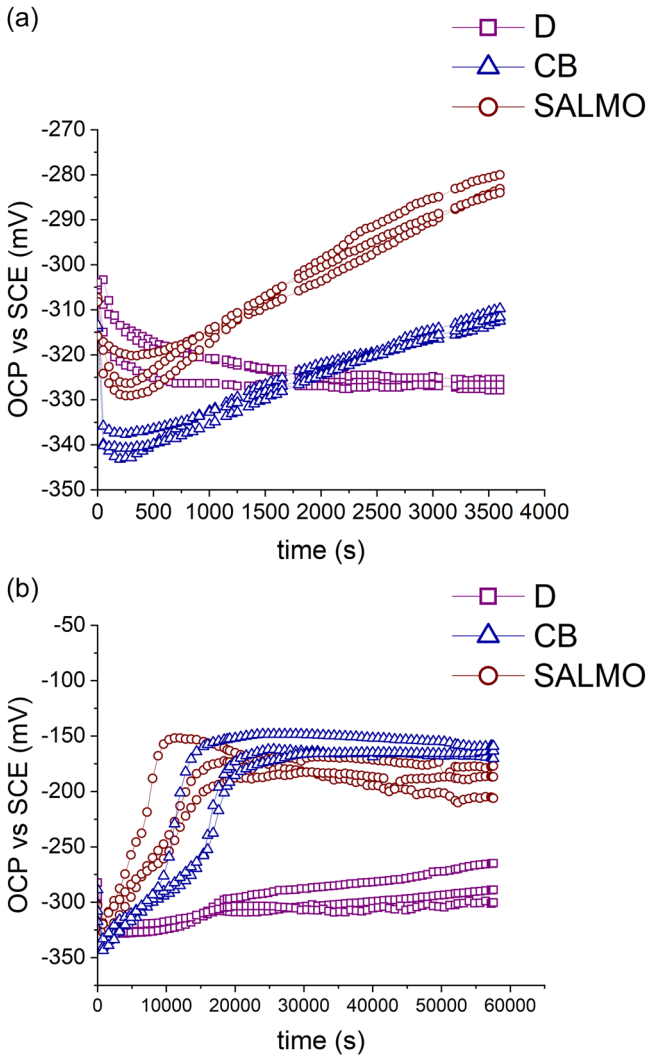

FIGURE 1 Open circuit potential (OCP) versus time curves for CuZn37 exposed for 1 h (a) and 16 h (b) to Darvell (D), Carter-Brugirard (C-B), and SALMO. Three independent measurements for each solution were performed.

Immediately upon exposure of the brass samples to the artificial saliva solutions, the OCP slightly decreased reaching a minimum after a few minutes (Figure 1a) suggesting the dissolution of the thin film formed during

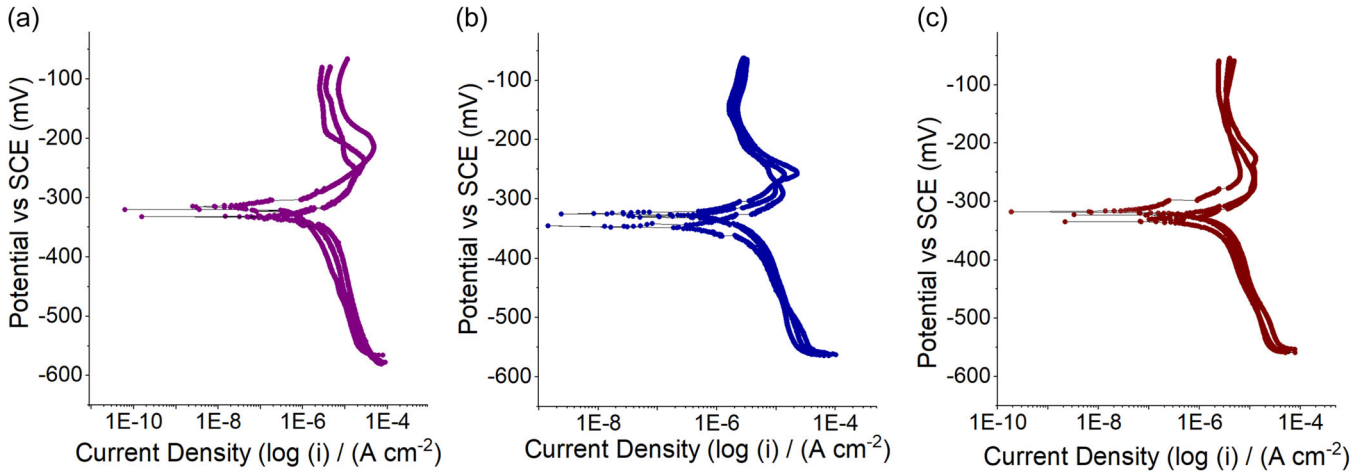

FIGURE 2 Potentiodynamic polarization curves of CuZn37 after 1 h of contact to (a) Darvell (D), (b) Carter-Brugirard (C-B), and (c) SALMO. Three independent measurements for each solution were performed.

TABLE 2 Average values of polarization resistance (*R*p) at various exposure times for each model solution

Model solutions	Rp_{1h} (kΩ cm^2)	Rp_{3h} (kΩ cm^2)	Rp_{16h} (kΩ cm^2)
Darvell	4.8 (0.6)	9 (4)	89 (6)
Carter-Brugirard	8 (1)	23 (10)	256 (41)
SALMO	16 (2)	136 (54)	338 (79)

Note: Standard deviations are given in parentheses.

mechanical polishing. For samples exposed to C-B and S solutions, the OCP then markedly increased for about 4h, reached a plateau after about 7 h and remained almost constant at OCP values of −150 mV SCE for C-B and about −200 mV SCE for S solution up to 16h (Figure 1b and Table 1). In the case of brass samples exposed to D formulation, the OCP increases only slightly and reaches about −300 mV SCE after 16 h of exposure (Figure 1b and Table 1).

3.4 | Potentiodynamic polarization curves

The polarization curves of brass samples in all saliva solutions tested (Figure 2) showed a cathodic branch, an active-passive transition, and an anodic region. The cathodic Tafel region showed βc values of −195 (22) mV/dec for C-B, −207 (10) mV/dec for S, and −206 (14)mV/dec for D, respectively, thus quite similar. The anodic Tafel slopes βa were estimated to be equal to 60 mV/dec. This allowed calculating the coefficient *B* according to the below equation:

$$B = \frac{\beta a \beta c}{2.303(\beta c + \beta a)}. \quad (1)$$

B values were found within the uncertainty of 20 (2) mV for the three artificial saliva solutions D, C-B, and S.

After the current maximum, an anodic plateau follows; the current density for C-B and S were in the range of 1.5–2.5 μA/cm^2, and the brass sample in the saliva D showed a much higher current density of 7–8 μA/cm^2 than in the other formulations.

3.5 | LPR and corrosion rate

LPR measurements were performed at the end of the OCP measurements for each exposure period of 1, 3, and 16 h. The LPR plots measured (not shown) in saliva solutions are curves characterized by a linear region at ±20 mV around the OCP. The *R*p values were determined by calculating the slope of the linear region. The average *R*p values and standard deviation for the different saliva solutions and the different exposure times are summarized in Table 2. The *R*p values increased with time of exposure and were the lowest for the D solution. From the *R*p measurements, the corrosion current density (i_{corr}) was estimated applying the Stern–Geary equation,[23] with the constant *B* determined experimentally by potentiodynamic polarization measurements.

The corrosion rates v_{corr} were determined for the different model solutions at the various exposure times by using Faraday's law; the average values and standard deviation are reported in Table 3. The corrosion rates

decreased over time and were the highest for the D solution.

4 | DISCUSSION

4.1 | Effect of exposure time

The OCP at initial time E_0 is about −301 (12) mV for brass in all solutions, then it decreased upon exposure to saliva solutions and reached a minimum after a few minutes (Figure 1). This initial behavior might indicate the dissolution of the surface film formed during mechanical polishing.[22] For prolonged exposure time, the OCP increased, becoming more positive in all model solutions (Figures 1b and 3a). The increase of the OCP in C-B and S solutions was similar to the results observed after contact of CuZn37 with the Tani-Zucchi formulation,[2] the OCP in the D solution reached much lower values than in the other cases (Table 1 and Figure 3a).

The *R*p markedly increased with exposure time for CuZn37 in contact with the saliva solutions (Figure 3b) and after 16 h of immersion the value is about 20 times higher than the initial one, indicating a decrease in the corrosion rate for prolonged exposure time. This behavior is probably due to the formation of a protective film.

TABLE 3 Average values of corrosion rate (v_{corr}) at various exposure times for each model solution

Model solutions	v_{corr1h} (μm/year)	$v_{corr\ 3h}$ (μm/year)	$v_{corr\ 16h}$ (μm/year)
Darvell	48 (11)	27 (12)	3.0 (0.3)
Carter-Brugirard	30 (8)	10 (5)	0.9 (0.2)
SALMO	15 (2)	1.8 (0.7)	0.8 (0.2)

Note: Standard deviations are given in parentheses.

4.2 | Dissolution mechanism

To propose the electrochemical mechanism of dissolution of the CuZn37 alloy in artificial saliva, a log *R*p versus OCP plot is presented (Figure 4). The exponential increase of *R*p with the OCP (straight line in the log *R*p vs. OCP diagram) is similar for all the model solutions here examined, and also for the Tani-Zucchi solution studied in previous works.[2–6]

The values measured for short immersion times (1 h) are found at low OCP and *R*p values, following the diagonal line the immersion time increases. A significant variation is found for values measured after 3 h for the Tani-Zucchi solution and the S solution. The slope

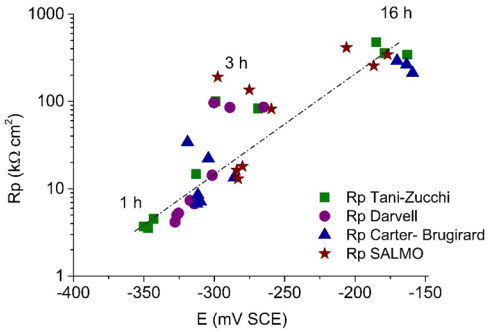

FIGURE 4 Diagram log *R*p versus OCP for CuZn37 alloy exposed for 1, 3, and 16 h to Darvell, Carter-Brugirard, and SALMO. For comparison, the results previously obtained with Tani-Zucchi saliva[2,3] are also reported. Three independent measurements for each solution were performed. *R*p, resistance potential; OCP, open circuit potential.

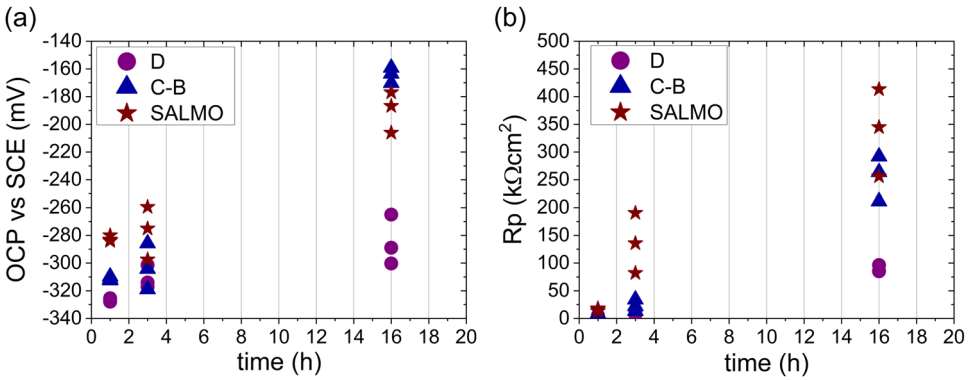

FIGURE 3 (a) Open circuit potential (OCP) versus time and (b) polarization resistance (*R*p) versus time for CuZn37 exposed for 1, 3, and 16 h to Darvell (D), Carter-Brugirard (C-B), and SALMO. Three independent measurements for each solution were performed.

of the line $\Delta\log Rp/\Delta OCP$ is positive and about 120 mV decade^{-1}.

Based on these results, it can be concluded that the dissolution of the CuZn37 alloy in all saliva solutions tested is the same and it is under anodic control. Therefore, the rate of the anodic reaction decreases with immersion time because a protective film is formed on the sample surface, which prevents or slows down the dissolution of the CuZn37 alloy. The results obtained in this study are in agreement with the literature[2–6]: the authors demonstrated[6] by the electrochemical impedance spectroscopy (EIS) measurements, performed on different brass alloys in contact with artificial saliva, that the corrosion rate is limited by the surface film formed as a result of the alloy dissolution.

4.3 | Influence of saliva composition

The increase of OCP and Rp values is less pronounced for the D solution in comparison with the other formulations; after 16 h the OCP reaches −285 (18) mV SCE and *Rp* was found to be 89 (6) kΩ cm^2. In addition, the anodic current density in the plateau region is much higher in the D solution (Figure 2). This behavior can be correlated with the presence of different organic substances: C-B contains only urea, S contains urea and glycine, instead in D solution in addition to urea, uric acid, lactic acid, and citric acid are also present. Despite the low concentration of these components (Supporting Information: Table S.1), their presence might influence the brass dissolution and the corrosion rate.

The Tani-Zucchi artificial saliva contains 0.1 g dm^{-3} of urea as an organic compound; previous XPS surface analysis studies of CuZn37 exposed to Tani-Zucchi solution[2–6] reported the formation of a protective film mainly composed of CuSCN and $Zn_3(PO_4)_2$ on the surface. This film was considered responsible for the lower dissolution rate of the alloy.

In this study, the XPS survey spectra recorded after immersion of brass into the saliva solutions (Figure 5) showed on all samples the presence of sulfur signals at 163 eV and S 2s at 227 eV, instead only on CuZn37 exposed to C-B and S solutions, the phosphorus signals (P 2p at 134 eV and P 2s at 192 eV) were revealed (Figure 5) despite a similar phosphate ion content in all the saliva formulations. The absence of phosphorus signals in the XPS survey spectra (Figure 5) and also in the detailed scans (not shown) on CuZn37 exposed to Darvell solution allowed excluding the precipitation of zinc phosphate on the sample surface. The absence of the zinc phosphate

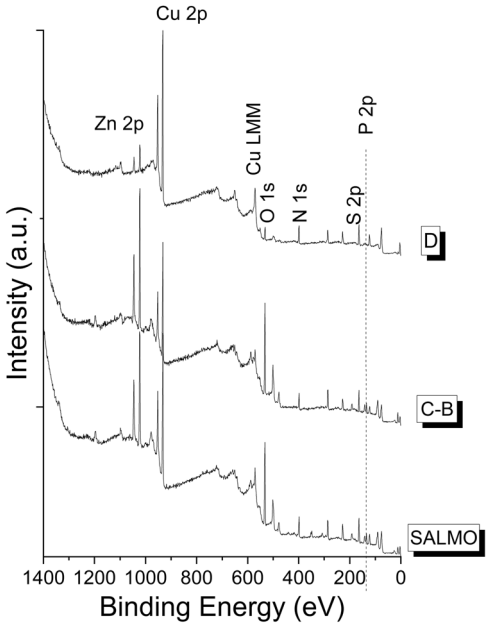

FIGURE 5 Survey spectra of X-ray photoelectron spectroscopy of CuZn37 alloy exposed for 1 h to Darrel (D), Carter-Brugirard (C-B), and SALMO

film can be explained by taking into account that the organic compounds, only present in the D solution, could act as complexing agents (e.g., citrate) for Zn, thus preventing its precipitation as phosphate. This hypothesis seems to be substantiated also by the marked decrease of Zn2p intensity in the survey spectra of CuZn37 exposed to D (Figure 5). The protective film in this case mainly consists of copper-thiocyanate species.

4.4 | Practical implications - corrosion rate

The corrosion current density (i_{corr}) showed the highest value after 1 h of immersion in saliva solutions and decreased upon increasing the exposure time (Figure 6). After 16 h of immersion, the corrosion current density was lower and the value was between 0.05 and 0.1 μA cm^{-2}. Calculating the corrosion rate using Faraday's law, the proportionality factor found is 12 (i.e., 1 μA cm^{-2} corresponds to 12 μm of section loss per year). The CuZn37 alloy exposed to the D solution showed the highest corrosion rate values after 16 h of immersion, while the S solution exhibited values approximately three times lower (Table 3).

In the case of brass alloys used for musical instruments, where brass/saliva contact can occur when musicians play the instruments, it can, therefore, be

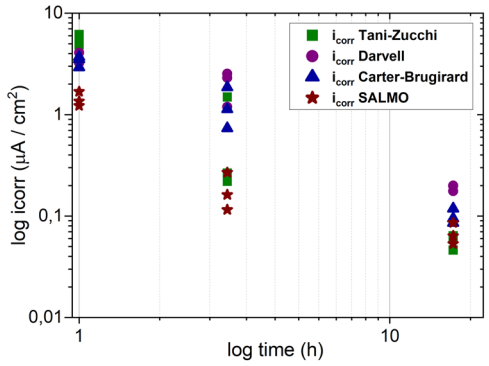

FIGURE 6 Corrosion density i_{corr} for CuZn37 alloy exposed for 1, 3, and 16 h to Darvell, Carter-Brugirard, and SALMO. For comparison, the results previously obtained with Tani-Zucchi saliva[2,3] are also reported. Three independent measurements for each solution were performed.

concluded that even if the liquid inside the instrument has a composition similar to that of one of the model solutions used in this study, corrosive attacks could only occur after years of use of the instrument. It should also be noted that these corrosion rate values were measured on CuZn37 alloys after mechanical polishing. The presence of a natural protective film slows down the dissolution.

5 | CONCLUSIONS

The composition of the artificial saliva solutions has a significant influence on the behavior of brass with respect to corrosion phenomena:

- OCP and *R*p measurements performed on CuZn37 brass samples after mechanical cleaning and in contact for 1, 3, and 16 h with the different model solutions (D, C-B, and S) showed that the dissolution mechanism is the same for all formulations and it is under anodic control.
- The corrosion rate (μm/year) v_{corr} significantly decreases upon the exposure time for all solutions and varies in the order: D> C-B> S.
- The corrosion rate trend can be correlated with the composition of the different model solutions. D solution differs in composition having various organic compounds: urea, lactic acid, uric acid, and citric acid.
- The presence of the different organic compounds in D formulation influences the composition of the surface film. The absence of the phosphorus signal in the contact area allows excluding the precipitation of zinc phosphate, which, in addition to CuSCN, was found to play a protective role against further corrosion of brass.

ACKNOWLEDGMENTS

Ministero dell'Università e della Ricerca, the Università di Cagliari, and Regione Autonoma della Sardegna are acknowledged for the financial support (POR FSE 2014/2020). The authors are grateful to UNICA-FdS (Fondazione di Sardegna) 2019—CUPF72F20000240007.

CONFLICT OF INTEREST

The authors declare no conflict of interest.

DATA AVAILABILITY STATEMENT

The data that support the findings of this study are available from the corresponding author upon reasonable request.

ORCID

Bernhard Elsener http://orcid.org/0000-0002-6855-1584
Antonella Rossi http://orcid.org/0000-0002-5151-2634

REFERENCES

[1] B. Elsener, M. Pisu, M. Fantauzzi, D. Addari, A. Rossi, *Mater. Corros.* **2016**, *67*, 591.
[2] F. Cocco, M. Fantauzzi, B. Elsener, A. Rossi, *RSC Adv.* **2016**, *6*, 90654.
[3] F. Cocco, *PhD thesis*, Università di Cagliari (Cagliari, Italy) **2016**.
[4] B. Elsener, F. Cocco, M. Fantauzzi, S. Palomba, A. Rossi, *Mater. Corros.* **2016**, *67*, 1336.
[5] B. Elsener, M. Alter, T. Lombardo, M. Ledergerber, M. Wörle, F. Cocco, M. Fantauzzi, S. Palomba, A. Rossi, *Microchem. J.* **2016**, *124*, 757.
[6] M. Fantauzzi, B. Elsener, F. Cocco, C. Passiu, A. Rossi, *Front. Chem.* **2020**, *8*, 272.
[7] J. Pytko-Polonczyk, A. Jakubik, A. Przeklasa-Bierowiec, B. Muszynska, *J. Physiol. Pharmacol.* **2017**, *68*, 807.
[8] V. W. Leung, B. W. Darvell, *J. Dent.* **1997**, *25*, 475.
[9] C. J. Dawes, *J. Dent. Res.* **1970**, *49*, 1263.
[10] I. R. Mandel, *J. Dent. Res.* **1974**, *53*, 246.
[11] M. Björklund, A. C. Ouwehand, S. D. Forssten, *Curr. Microbiol.* **2011**, *63*, 46.
[12] C. Llena-Puy, *Med. Oral Patol. Oral Cir. Bucal* **2006**, *11*, E449.
[13] G. Tani, F. Zucchi, *Minerva Stomatol.* **1967**, *16*, 710.
[14] B.W. Darvell, *J. Oral Rehabil.* **1978**, *5*, 41.
[15] M. Andrei, B. Galateanu, A. Hudita, M. Costache, P. Osiceanu, J. M. Calderon Moreno, S. I. Drob, I. Demetrescu, *Mater. Sci. Eng. C* **2016**, *59*, 346.
[16] F. Crea, C. De Stefano, D. Milea, A. Pettignano, S. Sammartano, *Bioinorg. Chem. Appl.* **2015**, *2015*, 267985.
[17] D. Biggio, M. Fantauzzi, B. Elsener, D. Atzei, A. Rossi, *Surface Interface Analysis*, **2022**, 1.

[18] S.L.R. Ellison, A. Williams, *Eurachem/CITAC guide: Quantifying Uncertainty in Analytical Measurement*, 3rd ed., Eurachem, Gembloux, Belgium **2012**.
[19] M. Crobu, *Master Thesis*, University of Cagliari (Cagliari, Italy) **2007**.
[20] M. Crobu, A. Scorciapino, B. Elsener, A. Rossi, *Electrochim. Acta* **2008**, *53*, 3364.
[21] VersaStudio 2.44.4, Princeton Applied Research, Ametek, **2015**.
[22] F. Cocco, B. Elsener, M. Fantauzzi, D. Atzei, A. Rossi, *RSC Adv.* **2016**, *6*, 31277.
[23] M. Stern, A.L. Geary, *J. Electrochem. Soc.* **1957**, *104*, 56.

SUPPORTING INFORMATION

Additional supporting information can be found online in the Supporting Information section at the end of this article.

How to cite this article: D. Biggio, B. Elsener, D. Atzei, A. Rossi, M. Fantauzzi, *Mater. Corros.* **2022**, 1–8. https://doi.org/10.1002/maco.202213476